Journal of Energy and Power Engineering 11 (2017) 372-379
doi: 10.17265/1934-8975/2017.06.002

Simulation of the Scattered EM Field of a Rotating Conducting Cylinder Using Static Data

Esmail M. M. Abuhdima and Robert P. Penno
Electrical Engineering, University of Dayton, Dayton, Ohio 45449, USA

Received: April 28, 2017 / Accepted: May 10, 2017 / Published: June 30, 2017.

Abstract: The effect of the rotation of a very good conducting cylinder on the backscattered field will be investigated where the incident wave is considered as a plane wave in both polarizations (E-wave and H-wave). Previous work has explained that rotation or vibration of the object may induce phase changes of the scattered signal. Modulation during rotation or vibration is referred to as micro-Doppler effect. Also, the effect of the rotation of a conducting cylinder was investigated by many researchers in the past using the Galilean transformation. These analyses conclude that the effect of rotation does not exist in the case of a perfectly conducting cylinder in both polarizations. In this work, the Franklin transformation is used instead of the Galilean transformation to analyze scattering of both types of electromagnetic waves (H-wave and E-wave) by rotating a very good circular conducting cylinder. This work shows that the scattered field is affected by the rotation of a very good conducting cylinder, especially in the case of H-wave (TE-mode). Finally, the model that will be presented is used to simulate rotation using static backscattered field data of an arbitrary object.

Key words: Backscattered field, conducting cylinder, rotation, translation.

1. Introduction

The special theory of relativity was used to discuss the scattering field of plane wave by a motion of the scatterer, where the scattered field is clearly affected by the translation motion of the body. In the case of the translation of the conducting cylinder, the special theory of relativity is the best method that was used to discuss the scattered fields and associated Doppler spectra [1, 2]. Since the rotating frame is the same as the instantaneous inertial frame in the definition of the special theory of relativity, this theory does not give the accurate analysis of the physics of rotation [3]. Many researchers in the past analyzed the effect of the rotation on the scattered field in terms of the Galilean transformation [4-6] and concluded that the effect of the rotation of the cylinder is negligible in the case of the perfect conductor. The capability of radars to describe the complex objects needs to improve, so it is very important to conduct the simulations that are used to characterize with higher fidelity the signal returned to a radar system from a moving complex object [7, 8]. Also, the measurement results [9] concluded that the strong "Doppler shifted" harmonics of the rotation frequency show up during the rotation of a smooth metallic cylinder, but it is required to have a mathematical expression to explain this phenomenon. In this work, the Franklin transformation is used to investigate the influence of the rotation of the conducting cylinder instead of Galilean transformation because the Franklin transformation gives accurate relation between the stationary frame and the rotating frame [10-12]. Also, the velocity of the rotating frame is defined as $v(r) = c\tanh(\Omega r/c)$, where Ω is the angular velocity of the rotation and c is the speed of light. Here, for the scattering of both types of polarization (E-wave and

Corresponding author: Esmail M. M. Abuhdima, Ph.D., research fields: wave propagation, electromagnetic field theory, antenna and simulation of radar signals.

H-wave) by a uniform rotating very good conducting cylinder is analyzed using Franklin transformation and the possible effects of the acceleration of the complex object on the scattered fields are investigated as well. The relations between the fields in both frames (laboratory frame and rotating frame) are found using Franklin transformation. The field inside the conducting cylinder and the changing in the surface current must be calculated to understand the behavior of the scattered fields of the rotating conducting cylinder. However, the jump in the tangential magnetic field at the surface of the conducting cylinder must be taken into account to investigate the change in the surface current that helps to describe the behavior of the scattered field during the rotation. Finally, the comprehensive electromagnetic simulation software tool for the electromagnetic field analysis of 3D structures (FEKO) is used to generate the static backscattered data of the complex object, and then these data will be inserted into the proposed model to simulate rotation.

2. Scattering by a Rotating Cylinder

In this section, the scattering of both types of electromagnetic plane waves by a rotating very good conducting cylinder is discussed herin. It is more convenient to use Maxwell's equations and the Franklin transformation in cylindrical form, (r, ϕ, z, t) in the laboratory frame and (r', ϕ', z', t') in the instantaneous inertial frame, where t is the time. The Franklin transformation is defined as [13].

$$r' = r\ ,\ \ \phi' = \phi\cosh(\beta) - \frac{ct}{r}\sinh(\beta) \tag{1}$$

$$z' = z\ ,\ \ t' = t\cosh(\beta) - \frac{r\phi}{c}\sinh(\beta) \tag{2}$$

where, $\beta = \Omega r/c$. It is assumed that $v_\phi = c\tanh(\beta)$, where v_ϕ is the velocity of the conducting cylinder in the ϕ direction. Since the constitutive equations and the boundary conditions at $r = a$ are affected by the rotation of the conducting cylinder, the relations between the electromagnetic components E, D, H, B in the laboratory frame can be written as Ref. [14].

$$D + \frac{v}{c}\times H = \varepsilon\left(E + \frac{v}{c}\times B\right) \tag{3}$$

$$B - \frac{v}{c}\times E = \mu\left(H - \frac{v}{c}\times D\right) \tag{4}$$

Substituting the velocity $v_\phi = c\tanh(\beta)$ into Eqs. (3) and (4) with $s = \tanh(\beta)$ gives

$$D_\phi = \varepsilon E_\phi$$

and

$$B_\phi = \mu H_\phi \tag{5}$$

$$D_r = \varepsilon a_s E_r + b_s H_z$$

and

$$B_r = \mu a_s H_r - b_s H_z \tag{6}$$

$$D_z = \varepsilon a_s E_z - b_s H_r$$

and

$$B_z = \mu a_s H_z + b_s E_r \tag{7}$$

While current densities are given as

$$J_r = \sigma\gamma\left(E_r + \mu s B_z\right) \tag{8}$$

$$J_z = \sigma\gamma\left(E_z - \mu s B_r\right) \tag{9}$$

$$J_\phi = \sigma\gamma^{-1}E_\phi \tag{10}$$

with the following notations

$$s = \tanh(\beta),\ \ \gamma = \left(1 - s^2\right)^{-1/2},$$

$$N^2 = \varepsilon_r\mu_r\ ,\ \ m^2 = N^2 - 1,$$

$$a_s = \left(1 - s^2\right)\left(1 - N^2 s^2\right)^{-1},$$

$$b_s = m^2 s\left(1 - N^2 s^2\right)^{-1},\ \ q = \frac{\sigma}{\varepsilon\omega},\ \ \alpha^2 = 1 - jq\ ,$$

where ε, μ, σ are the permittivity, permeability and conductivity of the material of the conducting rotating

cylinder. It is assumed that the material of the conducting cylinder is a non dispersive material. Also it is well known that the boundary conditions at $r = a$ can be written in Refs. [5, 6, 15]:

$$\bar{u}_r.\left(\bar{D}^{sc}+\bar{D}^{i}-\bar{D}\right)=\rho_s \tag{11}$$

$$\bar{u}_r\times\left(\bar{E}^{sc}+\bar{E}^{i}-\bar{E}\right)=0 \tag{12}$$

$$\bar{u}_r.\left(\bar{B}^{sc}+\bar{B}^{i}-\bar{B}\right)=0 \tag{13}$$

$$\bar{u}_r\times\left(\bar{H}^{sc}+\bar{H}^{i}-\bar{H}\right)=\bar{J}_s \tag{14}$$

where, the superscript "*sc*" indicates the scattered fields, "*i*" indicates the incident fields and the fields inside the conducting material without superscript.

2.1 Scattering by an E-wave (TM-Mode)

Fig. 1 shows a rotating circular conducting, cylinder with the radius, a, illuminated by an incident electrical field that is defined as Ref. [16].

$$E_z^{\,i}=e^{-jkx}=\sum_{-\infty}^{+\infty}j^{-n}J_n\left(kr\right)e^{jn\varnothing} \tag{15}$$

where, k=ω/c is the wave number. The Maxwell's equations inside the cylinder are [4]:

$$\frac{c}{r}\frac{\partial E_z}{\partial\varnothing}=-j\,\omega B_r \tag{16}$$

$$\frac{\partial E_z}{\partial r}=j\,\omega c^{-1}B_{\varnothing} \tag{17}$$

$$\frac{c}{r}\frac{\partial\left(rH_{\varnothing}\right)}{\partial r}-\frac{c}{r}\frac{\partial H_r}{\partial\varnothing}=j\,\omega D_z+J_z \tag{18}$$

Substituting Eqs. (5)-(10) into Eqs. (16)-(18) leads to Eq. (19) as

$$\frac{1}{r}\frac{\partial}{\partial r}\left(r\frac{\partial E_z}{\partial r}\right)+\left(\gamma_n^{\,2}-\frac{n^2}{r^2}\right)E_z=0 \tag{19}$$

where,

$$\gamma_n^{\,2}=k^2N^2\left(1-jq\right)+\frac{n\,\omega\Omega}{c^2}\left(2N^2-2-jN^2q\right)\cdot$$

Since Eq. (19), which defined the field inside the conducting cylinder, is the Bessel type equation, so its solution is given as Ref. [17].

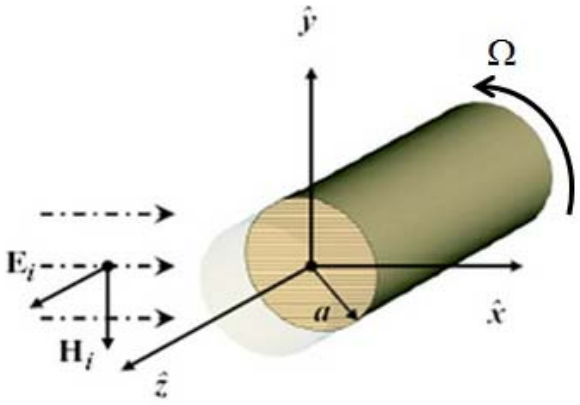

Fig. 1 Rotating conducting cylinder illuminated by E-wave.

$$E_Z=\sum_{-\infty}^{+\infty}A_nJ_n\left(\gamma_nr\right)e^{jn\varnothing} \tag{20}$$

The scattered field can be written as

$$E_z^{\,sc}=\sum_{-\infty}^{+\infty}B_nH_n^{(2)}\left(kr\right)e^{jn\varnothing} \tag{21}$$

where, A_n and B_n are the unknown amplitude coefficients. The boundary conditions that is defined in Eqs. (12) and (14) are used to find these two coefficients as

$$B_n=\frac{j^{-n}\left[c\gamma_nJ_n^{'}\left(\gamma_na\right)J_n\left(ka\right)-kJ_n\left(\gamma_na\right)J_n^{'}\left(Ka\right)\right]}{kJ_n\left(\gamma_na\right)H_n^{\prime(2)}\left(Ka\right)-c\gamma_nJ_n^{'}\left(\gamma_na\right)H_n^{(2)}\left(ka\right)} \tag{22}$$

$$A_n=\frac{j^{-n}k\left[J_n^{'}\left(ka\right)H_n^{(2)}\left(ka\right)-J_n\left(ka\right)H_n^{\prime(2)}\left(Ka\right)\right]}{c\gamma_nJ_n^{'}\left(\gamma_na\right)H_n^{(2)}\left(ka\right)-kJ_n\left(\gamma_na\right)H_n^{\prime(2)}\left(Ka\right)} \tag{23}$$

The effect of the rotation of the conducting cylinder on the scattered fields is neglected in the case of the E-wave as shown in Eq. (22). When the conductivity (σ) is very large, Eq. (21) gives similar result as the scattered field from a stationary conducting cylinder [18], so Eq. (21) becomes

$$\lim_{\sigma\to large}\mathrm{E}_z^{sc}=\sum_{-\infty}^{+\infty}\frac{J_n\left(ka\right)}{H_n^{(2)}\left(Ka\right)}H_n^{(2)}\left(kr\right)e^{jn\varnothing} \tag{24}$$

It can conclude that the effect of the rotation is neglected up to $o(\beta)$ in the case of E-wave (TM-mode).

2.2 Scattering by an H-Wave (TE-Mode)

The time-harmonic incident field in an E-wave is shown in Fig. 2 and the incident magnetic field can be written as Ref. [16].

$$H_z^i = e^{-jkx} = \sum_{-\infty}^{+\infty} j^{-n} J_n(kr) e^{jn\varnothing} \tag{25}$$

Maxwell equations inside the cylinder are [5]

$$\frac{c}{r}\frac{\partial H_z}{\partial \varnothing} = J_r + j\omega D_r \tag{26}$$

$$-c\frac{\partial H_z}{\partial r} = J_\varnothing + j\omega D_\varnothing \tag{27}$$

$$\frac{c}{r}\frac{\partial (rE_\varnothing)}{\partial r} - \frac{c}{r}\frac{\partial E_r}{\partial \varnothing} = -j\omega B_z \tag{28}$$

The field inside the conducting cylinder and the scattered field can be written as

$$H_Z = \sum_{-\infty}^{+\infty} A_n J_n(\gamma_n r) e^{jn\varnothing} \tag{29}$$

$$H_z^{sc} = \sum_{-\infty}^{+\infty} B_n H_n^{(2)}(kr) e^{jn\varnothing} \tag{30}$$

Applying the boundary conditions that are defined in Eqs. (11)-(14) to find A_n and B_n as

$$B_n = \frac{\left[kJ_n'(ka)J_n(\gamma_n a)\left(\alpha^2\epsilon_r + n\frac{\Omega\epsilon_r}{\omega}\right) - c\gamma_n J_n(ka)J_n'(\gamma_n a)\left(1+n\frac{\Omega}{\omega c\epsilon_o}\right)\right]}{c\gamma_n J_n'(\gamma_n a)H_n^{(2)}(Ka)\left(1+n\frac{\Omega}{\omega c\epsilon_o}\right) - kJ_n(\gamma_n a)H_n'^{(2)}(ka)\left(\alpha^2\epsilon_r + n\frac{\Omega\epsilon_r}{\omega}\right)} \tag{31}$$

$$A_n = \frac{j^{-n}\left[J_n(ka)H_n'^{(2)}(ka)\left(\left(1+n\frac{\Omega}{\omega c\epsilon_o}\right)\right) - J_n'(ka)H_n^{(2)}(Ka)\left(1+n\frac{\Omega}{\omega c\epsilon_o}\right)\right]}{H_n'^{(2)}(ka) - J_n'(\gamma_n a)H_n^{(2)}(Ka)\left(1+n\frac{\Omega}{\omega c\epsilon_o}\right)\left(\frac{c\gamma_n}{k\alpha^2\epsilon_r}\right)} \tag{32}$$

The effect of the rotation of the conducting cylinder on the scattered field is clearly shown through the Ω terms as shown in Eq. (31). When the conductivity of the rotating cylinder is very large, the behavior of the scattered field during the rotation is different from the stationary case. To this end, the effect of the rotation is more evident in the case of the H-wave.

3. Proposed Model to Simulate Rotating Object

In this part, the model used to simulate rotation using backscattered field data will be designed. The characteristics of the electromagnetic scattering field from a rotating conducting circular cylinder were investigated using Franklin transformation [10]. Theoretical analysis indicated that the scattered field is affected by the rotation of the conducting cylinder in the case of H-wave. In the case of H-wave, the backscattered field Eq. (30) can be written as

$$\mathrm{H}_r^{sc} = \hat{z}\frac{e^{-jkr}}{\sqrt{r}}\frac{1}{\sqrt{\pi k}}\left[\sum_{-\infty}^{+\infty} B_n (1+j) e^{jn\pi}\right] \tag{33}$$

where, B_n is defined by Eq. (31). It is clear that the backscattered field is affected by the rotation proportional to the β_a. The backscattering of the H-wave by a stationary conducting cylinder is [18]

$$\mathrm{H}_s^{sc} = \hat{z}\frac{e^{-jkr}}{\sqrt{r}}\frac{1}{\sqrt{\pi k}}\sum_{-\infty}^{+\infty}(1+j)\frac{J_n'(ka)}{H_n^{(2)\prime}(Ka)}e^{jn\pi} \tag{34}$$

Eqs. (33) and (34) are used to find the relation between two cases as

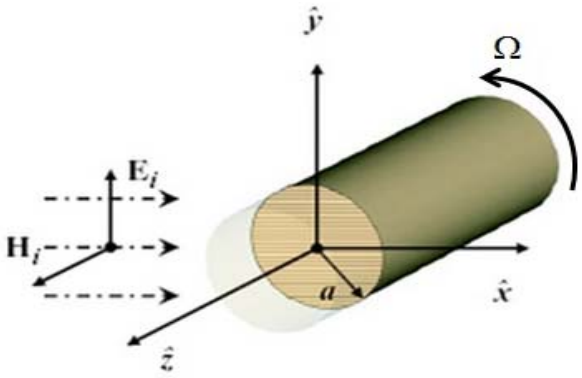

Fig. 2 Rotating conducting cylinder illuminated by H-wave.

$$\mathrm{H}_r^{\mathrm{sc}} = \mathrm{H}_s^{\mathrm{sc}} \times A(s) \tag{35}$$

and then

$$\sum_{-\infty}^{+\infty} B_n e^{jn\pi} = \left(\sum_{-\infty}^{+\infty} \frac{J_n'(ka)}{H_n^{(2)\prime}(Ka)} e^{jn\pi} \right) \times A(s) \tag{36}$$

where $A(s)$ is the relation between stationary and rotation case and it can be written as

$$A(s) = \frac{\sum_{-\infty}^{+\infty} B_n e^{jn\pi}}{\sum_{-\infty}^{+\infty} \frac{J_n'(ka)}{H_n^{(2)\prime}(Ka)} e^{jn\pi}} \tag{37}$$

where H_s^{sc} and H_r^{sc} are the backscattered field of the stationary and rotating object respectively. Here, FEKO is used to generate the static backscattered data of the complex object, and then these data will be inserted into the model to simulate rotation as shown in Fig. 3. The discussion of the output data is presented in the next section.

4. Numerical Results

This section includes two parts. The first one discusses the simulation of the scattered electromagnetic field from a rotating conducting cylinder in the case of an H-wave. The second part describes how the proposed model is used to simulate rotation. In the far field region for the case of rotation, the magnitude of the scattered field of a very good conducting cylinder

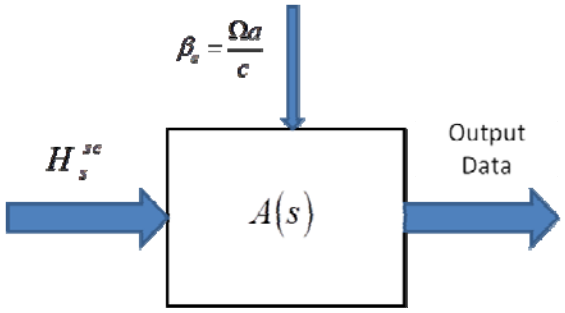

Fig. 3 Proposed model.

is shown in Fig. 4, where the distortion of the magnitude of the scattered field is clearly shown in Figs. 4 and 5. The effect of the rotation shows up with the shift of the primary lobe of the forward scattered field and the side lobes in the direction of the cylinder rotation. The effect of rotation of the conducting cylinder on the scattered field is not evident in terms of the Galilean transformation as shown in Figs. 4 and 5. When the values of the rotation are increased, the primary forward lobe is broken up and the side lobes are increased as shown in Fig. 5.

It is noted that at higher frequencies distinct difference exists between the backscattered field of the stationary cylinder and the rotating one, but this difference is very small at lower frequencies as shown in Fig. 6. Also, it is shown that the difference between the rotating field and stationary field is increased when the angular velocity or radius of the cylinder is increased [10].

Furthermore, the rotation produces a periodicity on the backscattered field when the incident frequency is greater than 10.8 GHz and a deep null occurs at 11.4 GHz. The phase of the backscattered field has the similar behavior as shown in Fig. 7. The difference in the phase is more distinct in the higher frequencies and this difference is increased when the angular velocity or radius of the cylinder is increased as well [11].

In the second part, FEKO is used to generate backscattered field data by a stationary conducting cylinder. The geometry of the complex object is shown in Fig. 2, which shows that the axis of the

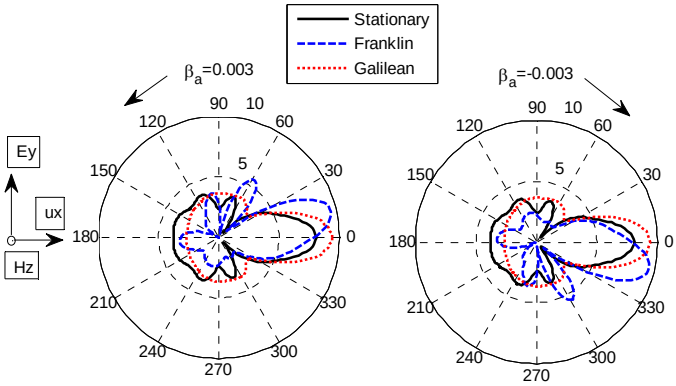

Fig. 4 The magnitude of the scattered field of very good conducting cylinder (σ = 5.76 × 10^7 s/m, a = 0.039 m, f = 5.8 GHZ).

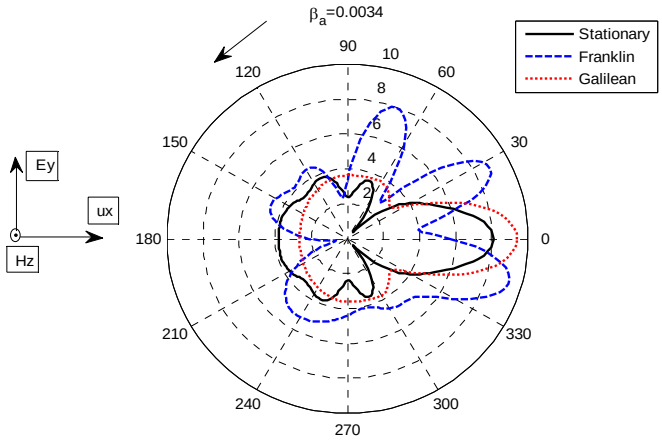

Fig. 5 The magnitude of the scattered field of very good conducting cylinder (σ = 5.76 × 10^7 s/m, a = 0.039 m, f = 5.8 GHZ).

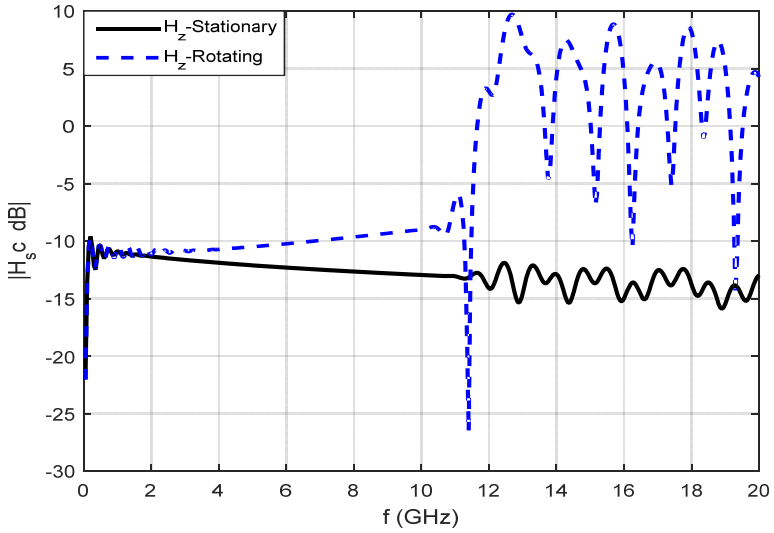

Fig. 6 Magnitude of the backscattered magnetic field as a function of frequency for a very good conducting cylinder, immersed in an incident H-wave (σ = 5.76 × 10^7 s/m, a = 0.2 m, β_α = 0.0009).

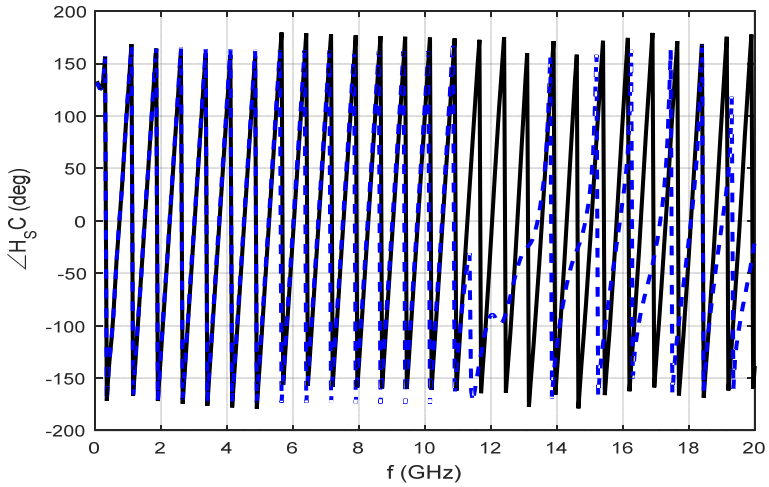

Fig. 7 Phase of the backscattered magnetic field as a function of frequency for a very good conducting cylinder, immersed in an incident H-wave ($\sigma = 5.76 \times 10^7$ s/m, $a = 0.2$ m, $\beta_a = 0.009$).

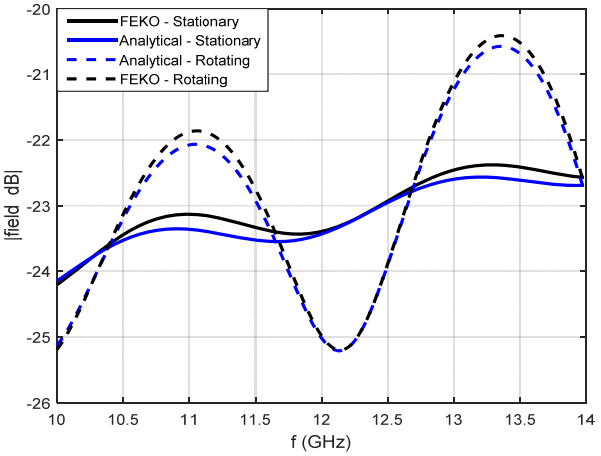

Fig. 8 Magnitude of the backscattered field.

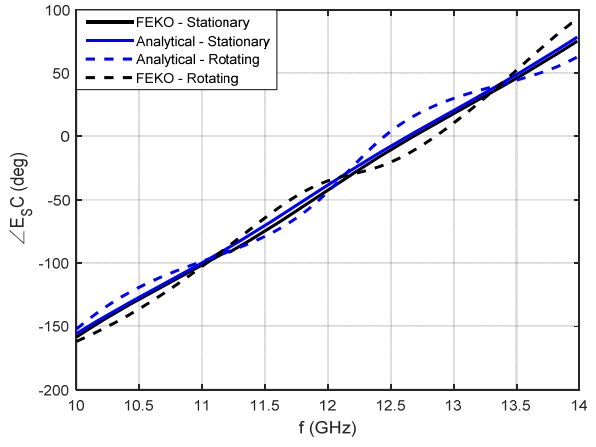

Fig. 9 Phase of the backscattered field.

cylinder is in *Z*-direction and the propagating plane wave in X-direction. Also, the electric field is polarized in the Y-direction (TE-mode). The radius of the cylinder is 0.025 m and its height is 0.10 m. The incident operating frequency changed from 10 GHz to 14 GHz. Fig. 8 shows the frequency dependence of the backscattered field for a conducting cylinder with higher conductivity. A comparison of the backscattered field that is investigated by using analytical method and the backscattered field using FEKO data reveals that the two methods give similar results. It is acceptable to see little difference between the two methods because the analytical method used an approximation to $o(\beta_a)$ to solve the sophisticated complex equations. Also, a comparison of Figs. 8 and 9 reveals that the phase patterns of the backscattered field show a sinusoidal behavior when the conducting cylinder is rotating with $\beta_a = 0.02$. The peak values of the sinusoidal behavior of the phase are related to the points where the amplitudes of the backscattered fields are equal in both cases (stationary and rotating) such as 10.39, 11.66 and 12.67 GHz as shown in Fig. 8. Also the peak values of the amplitudes of the backscattered fields are related to the points where the phases of the backscattered fields are equal, such as 11.11, 12.14 and 13.34 GHz as shown in Fig. 9. Further, the period of the sinusoidal behavior of the backscattered phase decreases when the rotation of the cylinder is increased.

5. Conclusions

The effect of rotation on both phase and magnitude of the scattered electromagnetic field from a very good conducting circular cylinder of infinite extent is investigated in this work. The Franklin transformation was used to investigate the scattered fields to the first order of the parameter, $\beta_a = \Omega a/c$, and showed significant deviations from the stationary case in both phase and magnitude of the scattered field, especially at higher frequencies. The numerical results indicate that the rotation of the conducting cylinder produced a shift on the phase of the backscattered field, which is often referred to as micro-Doppler shift. Further, the numerical results also proved that the Franklin transformation gives a more accurate analysis of rotation of a very good conducting cylinder than Galilean transformation. This paper introduced a model that is used to simulate rotation from statically derived data. It was seen that these simulated results corroborate the theoretical results of a rotating cylinder. Future work includes developing a model that is used to simulate the rotation and the translation of an arbitrary complex object using statically collected, scattered field data.

References

[1] De Zutter, D., and Van Bladel, J. 1977. "Scattering by Cylinders in Translational Motion." *IEEE Journal on Microwaves, Optics and Acoustics* 1 (6): 192-6.

[2] De Zutter, D. 1980. "Fourier Analysis of the Signal Scattered by Objects in Translational Motion, Part I and II." *Applied Scientific Research* 36 (4): 241-69.

[3] Gholizade, H. 2014. "Radar Cross Section of Moving Objects." *The European Physical Journal* arXiv:1306.4691.

[4] Hillion, P. 1998. "Scattering by a Rotating Circular Conducting Cylinder I." *Mathematical Physics* 41 (2): 223-33.

[5] Hillion, P. 1998. "Scattering by a Rotating Circular Conducting Cylinder II." *Mathematical Physics* 41 (2): 253-44.

[6] De Zutter, D. 1983. "Scattering by a Rotating Circular Cylinder with Finite Conductivity." *IEEE Transactions on Antenna and Propagation* AP-31 (1): 166-9.

[7] Harding, G., and Penno, R. 2014. "Dynamic Simulation of Electromagnetic Scattering from Complex Airborne Platforms." Presented at *IEEE Radar Conference*, Cincinnati, OH.

[8] Cammenga, Z. A., Baker, C. J., Smith, G. E., and Ewing, R. 2014. "Micro-Doppler Target Scattering." In *Proceedings of the IEEE International Radar*, 1451-5.

[9] Christensen, J. K., and Underhill, M. J. 2004. "Doppler Measurements of Smooth and Rough Surface High Frequency Scattering from Spinning Steel Cylinders." *IEEE A&E Systems Magazine* 19 (12): 11-4.

[10] Abuhdima, E., and Penno, R. 2015. "Simulation of the Scattered EM Fields from a Rotating Conducting Cylinder." In *Proceedings of the IEEE International Radar Conference,* 1078-83.

[11] Abuhdima, E., and Penno, R. 2015. "An Improved Model for the Phase of Backscattered Electromagnetic Fields from a Conducting Rotating Cylinder." In *Proceedings of the National Aerospace and Electronics Conference*, 183-7.

[12] Nouri-Zonoz, M., and Ramezani-Aval, H. 2014. "Fermi Coordinates and Modified Franklin Transformation: A Comparative Study on Rotational Phenomena." *The European Physical Journal C* 74 (10): 1-9.

[13] Franklin, P. 1922. "The Meaning of Rotation in the Special Theory of Relativity." *Proceedings of the National Academy of Sciences of the United States of America* 8 (9): 265-8.

[14] Hillion, P. 1998. "Scattering Maxwell's Equations and Accelerated Frames." *Physical Review E* 57 (6): 7239-43.

[15] Van Bladel, J. 1976. "Electromagnetic Field in the Presence of Rotating Bodies." *Proceedings of the IEEE* 64 (3): 301-18.

[16] Harrington. 1961. *Time Harmonic Elecromagnetic Fields*, McGraw-Hill, 234.

[17] Tai, C. T. 1964. *Two Scattering Problems Involving Moving Media*. Ohio State University Research Foundation Report, 1691-7.

[18] Balanis, C. A. 1989. *Advanced Engineering Electromagnetics.* Hoboken: John Wiley & Sons, Inc.